

MORPHOLOGICAL CONVERGENCE AND
DISPARITY IN THE EVOLUTION OF
TENRECS (AFROSORICIDA, TENRECIDAE)

by

SIVE FINLAY

B.A. (mod), Trinity College Dublin 2012

A thesis submitted in partial fulfillment of
the requirements for the degree of

MASTERS BY RESEARCH

School of Natural Sciences
(Zoology)

Trinity College Dublin

JANUARY 2015

© Sive Finlay, 2015

ABSTRACT

Here is the abstract of my thesis.

TABLE OF CONTENTS

| | |
|---|-----|
| ABSTRACT | ii |
| TABLE OF CONTENTS | iii |
| LIST OF TABLES | v |
| LIST OF FIGURES | vi |
| ACKNOWLEDGEMENTS | vii |
| 1 INTRODUCTION | 1 |
| 1.1 Patterns of morphological diversity | 1 |
| 1.2 Disparity | 1 |
| 1.3 Convergence | 2 |
| 1.4 Tenrecs | 2 |
| 1.5 Structure & contents of this thesis | 3 |
| 2 DATA COLLECTION AND PROCESSING | 4 |
| 2.1 Introduction | 4 |
| 2.2 Data collection | 5 |
| 2.2.1 Species measured and taxonomy | 5 |
| 2.2.2 Museum label data | 6 |
| 2.2.3 Linear measurements | 7 |
| 2.2.4 Photographic set up | 11 |
| 2.2.5 Photographing specimens | 12 |
| 2.2.6 Saving and processing images | 13 |
| 2.3 Geometric morphometric analyses | 14 |
| 2.3.1 Landmark placement on images | 14 |
| 2.3.2 Skulls: dorsal view | 15 |
| 2.3.3 Skulls: ventral view | 15 |
| 2.3.4 Skulls: lateral view | 17 |
| 2.3.5 Mandibles | 19 |
| 2.3.6 Procrustes superimposition | 21 |
| 2.4 Error checking | 22 |
| 2.4.1 Taxonomic | 22 |
| 2.4.2 Specimen ID | 23 |
| 2.4.3 Specimen sex and age | 23 |

| | | |
|----------|---|-----------|
| 2.4.4 | Linear measurements | 24 |
| 2.4.5 | Potential morphometrics error | 25 |
| 2.4.6 | Landmark placement | 26 |
| 3 | DISPARITY IN TENRECS COMPARED TO THEIR CLOSEST RELATIVES | 27 |
| 3.1 | Introduction | 27 |
| 3.2 | Methods | 27 |
| 3.3 | Results | 28 |
| 3.3.1 | Morphological disparity in tenrecs and golden moles . . . | 29 |
| 3.3.2 | Morphological disparity in non- <i>Microgale</i> tenrecs and golden moles | 31 |
| 3.4 | Discussion | 32 |
| 4 | CONVERGENCE AMONG TENRECS AND OTHER SMALL MAMMALS | 33 |
| 4.1 | Introduction | 33 |
| 4.2 | Methods | 33 |
| 4.2.1 | Phylogeny | 33 |
| 4.2.2 | Quantifying convergence | 34 |
| 4.3 | Results | 34 |
| 4.4 | Discussion | 34 |
| 5 | DISCUSSION | 35 |
| 5.1 | General discussion | 35 |
| 5.2 | Possible issues | 35 |
| 5.3 | Future directions | 35 |
| 5.3.1 | Measuring the adaptiveness of phenotypic traits | 35 |
| 5.3.2 | Evolutionary predictions of divergence and convergence . | 35 |
| 5.3.3 | Ecological convergence | 35 |
| 5.3.4 | Studies of behavioural convergence | 35 |
| 5.4 | Conclusions | 37 |
| | BIBLIOGRAPHY | 38 |

LIST OF TABLES

| | | |
|-----------|---|----|
| TABLE 2.1 | Species measured | 6 |
| TABLE 2.2 | Mandible measurements | 8 |
| TABLE 2.3 | Skull measurements | 9 |
| TABLE 2.4 | Limb measurements | 10 |
| TABLE 2.5 | Skulls: dorsal landmarks | 17 |
| TABLE 2.6 | Skulls: ventral landmarks | 18 |
| TABLE 2.7 | Skulls: lateral landmarks | 19 |
| TABLE 2.8 | Mandibles: landmarks | 21 |
| TABLE 3.1 | Comparisons of morphospace occupation by tenrecs and golden moles (npMANOVA) | 30 |
| TABLE 3.2 | Comparisons of disparity metrics for tenrecs and golden moles | 31 |
| TABLE 3.3 | Comparisons of disparity metrics for non- <i>Microgale</i> tenrecs and golden moles | 32 |

LIST OF FIGURES

| | |
|---|----|
| FIGURE 2.1 Examples of museum labels | 7 |
| FIGURE 2.2 Photographic set up | 12 |
| FIGURE 2.3 Skulls: dorsal landmarks | 16 |
| FIGURE 2.4 Skulls: ventral landmarks | 17 |
| FIGURE 2.5 Skulls: lateral landmarks | 19 |
| FIGURE 2.6 Mandibles: landmarks | 21 |
| FIGURE 3.1 Principal components plots of the morphospaces occupied by tenrecs and golden moles | 29 |

ACKNOWLEDGEMENTS

I would like to acknowledge Dr Rich FitzJohn for letting me use his thesis template!

CHAPTER 1

INTRODUCTION

1.1 PATTERNS OF MORPHOLOGICAL DIVERSITY

Patterns of diversity,
morphological differences,
geometric morphometrics overview

1.2 DISPARITY

There are many famous examples of adaptively radiated groups (Gavrilets and Losos, 2009). However, there has also been considerable debate about how adaptive radiations should be defined (Glor, 2010; Losos and Mahler, 2010) based on the relative importance of speciation rate, species richness and morphological diversity. One particular issue is whether it is even meaningful to classify a particular group of species as an adaptive radiation or not since any classification relies on arbitrary distinctions between what is most likely a continua of characteristics which describe the diversity of a particular clade (Olson and Arroyo-Santos, 2009).

However, despite the controversies and disagreements, there does seem to be a consensus that high morphological diversity is an important criteria for identifying a group of species as belonging to the adaptive radiation scale (Losos and Mahler, 2010; Olson and Arroyo-Santos, 2009). One way to test

whether a group shows high morphological diversity is through sister taxa comparisons. For example, Losos and Miles (2002) used this approach to demonstrate exceptional diversity in some but not all clades of iguanid lizards.

1.3 CONVERGENCE

Long history of study

Repeatability of evolution

Methods of measuring convergence

1.4 TENRECS

The tenrec family is comprised of 34 species, 31 of which are endemic to Madagascar (Olson, 2013). From a single common ancestor (Asher and Hofreiter, 2006), Malagasy tenrecs diversified into a wide variety of descendant species which convergently resemble distantly related insectivore mammals such as shrews (*Microgale* tenrecs), moles (*Oryzorictes* tenrecs) and hedgehogs (*Echinops* and *Setifer* tenrecs) (Eisenberg and Gould, 1969). These convergent resemblances are so great that tenrecs used to be considered part of the general "insectivore" clade and only molecular studies revealed their true phylogenetic affinities within the Afrotherian mammals (Stanhope *et al.*, 1998).

Tenrecs are often cited as an example of an adaptively radiated family which exhibits exceptional morphological diversity (Soarimalala and Goodman, 2011; Olson and Goodman, 2003; Eisenberg and Gould, 1969). However, this apparent exceptional diversity is based on subjective comparisons to other groups and it has not been tested. Here we present the first quantitative test of patterns of phenotypic diversity in tenrecs and examine how morphological diversity in tenrecs compares to their closest relatives, the golden moles (Afrosoricida, Chryschloridae).

Tenrecs are also considered to be a clade which is highly convergent with other small mammal species ...

1.5 STRUCTURE & CONTENTS OF THIS THESIS

In this thesis I quantify patterns of phenotypic diversity within tenrecs (chapter 3) and morphological convergence among tenrecs and other small mammals (chapter 4). In chapter 2 I describe the data collection and general analyses which form the basis for my studies of disparity and convergence. These analyses are the first systematic and quantitative studies of patterns of phenotypic diversity in the tenrec family and I discuss their implications in chapter 5. My results reveal new insights into our understanding of morphological variety in tenrecs and prompt many new questions and possible avenues for further research.

CHAPTER 2

DATA COLLECTION AND PROCESSING

2.1 INTRODUCTION

I compiled a morphological data set of both photographs and linear measurements from 366 specimens representing 99 species of small mammals. I collected morphological data from skulls, limbs and skins. I have only analysed the skulls' data in detail so the information I collected on limbs and skins represent significant resources for future work.

I have divided my description of how the data were collected and analysed into three sections:

i Data collection (section 2.2):

Summary of the species measured, information recorded from the museum labels, linear measurements and photographic set up.

ii Geometric morphometric analyses (section 2.3):

Landmark and semilandmark placement on different views of skulls and mandibles.

iii Error checking (section 2.4):

How I dealt with errors in taxonomic and specimen identification, possible variation associated with sex and age class, accuracy and repeatability of linear measurements and morphometric errors associated with photographing specimens and the placement of landmarks.

2.2 DATA COLLECTION

2.2.1 Species measured and taxonomy

Between January and September 2013, I spent a total of 9 weeks working in the collections of five museums: the Natural History Museum London (NHML), the Smithsonian Institute Natural History Museum (SI), the American Museum of Natural History (AMNH), Harvard's Museum of Comparative Zoology (MCZ) and the Field Museum of Natural History (FMNH), Chicago. I measured and photographed 366 skulls, 248 post-cranial skeletons and 277 skins from 101 species belonging to four mammalian Orders; Afrosoricida, Erinaceomorpha, Soricomorpha and Notoryctemorphia. These belonged to seven families of mammals; tenrecs (Tenrecidae), golden moles (Chrysochloridae), hedgehogs and gymnures (Erinaceidae), shrews (Soricidae), solenodons (Solenodontidae), moles and desmans (Talpidae) and marsupial moles (Notoryctidae). I measured all of the tenrecs and their sister taxa the golden moles that were available in the collections (31 species of tenrec, 12 species of golden moles, table 2.1).

For my comparative species of non-Afrosoricida species, I chose a random sample of 56 taxa which have been previously identified as convergent with tenrecs (e.g. Gould and Eisenberg, 1966; Symonds, 2005; Poux *et al.*, 2008; Olson, 2013). Following the taxonomy in Wilson and Reeder's Mammal Species of the World (MSW) (2005), I used phylogenies for each Order to select species at random which represented the main sub-branches and morphological diversity of each Order. For example, within the Soricomorpha, I only included 3 species of *Crocidura* (out of a total of 230, Wilson and Reeder 2005) but both species of the *Solenodon* Genus because it represents a separate subgroup to the rest of the Order.

I used the taxonomy of Wilson and Reeder's Mammal Species of the World (MSW, 2005) supplemented with more recent sources (e.g. Olson, 2013; Soarimalala and Goodman, 2011) to identify the specimens. Table 2.1 outlines the

number of species I measured from each Family and how this sample relates to the overall number of species in that group as recorded by MSW (2005).

TABLE 2.1: The number of species I measured in each Family compared to the total number of species in that Family according to Wilson and Reeder's Mammal Species of the World 2005

| Order | Family | Species measured | Species in MSW |
|------------------|-----------------|-------------------------|-----------------------|
| Afrosoricida | Tenrecidae | 31 | 30 |
| Afrosoricida | Chrysochloridae | 12 | 21 |
| Erinaceomorpha | Erinaceidae | 16 | 24 |
| Soricomorpha | Soricidae | 22 | 376 |
| Soricomorpha | Solenodontidae | 2 | 4 |
| Soricomorpha | Talpidae | 15 | 39 |
| Notoryctemorphia | Notoryctidae | 1 | 2 |

Wilson and Reader (2005) record 30 species of tenrec but more recent studies indicate that there are now 34 species(Olson, 2013). The additional species belong to the shrew tenrec (*Microgale*) Genus and represent either recognition of cryptic species boundaries (Olson *et al.*, 2004) or discovery of new species (Goodman *et al.*, 2006; Olson and Arroyo-Santos, 2009). Only one of these four recent additions, *M. jobihely*, was present in the museum collections and therefore I could not include the three other newly recognised species in my analyses.

2.2.2 Museum label data

I recorded all the data on the specimen labels including any handwritten or printed notes which had been added by other users of the collection. The label data included the museum specimen ID number, Genus, species, sex, collector's name, the date and location of collection. Some of the labels attached to skins had additional information such as the body, tail, hind foot and ear lengths as well as the body mass of the live individual. The level of detail recorded on the labels varied considerably (figure 2.1). For example recently

collected specimens were more likely to have detailed information about the collection location, and some specimens did not have even basic information such as the sex recorded.

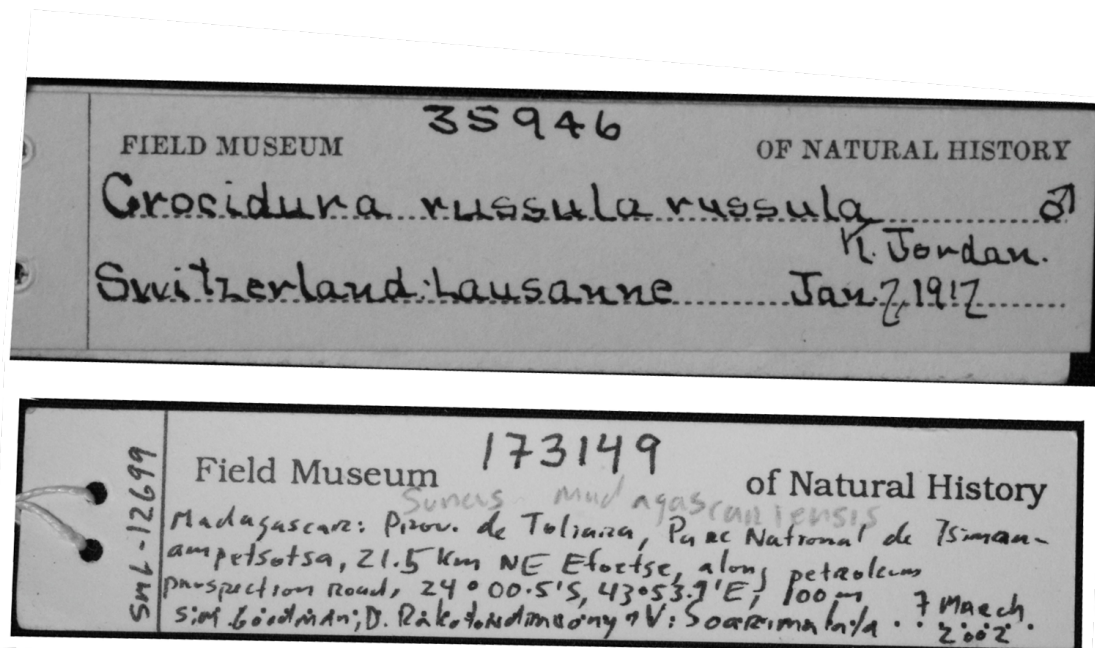


FIGURE 2.1: Examples of the variation in the detail of information which is available from museum labels.

2.2.3 Linear measurements

Using a 15mm digital calipers (Mitutoyo Absolute digimatic calipers), I took 5 measurements of the mandibles (table 2.2, 15 of the skulls (table 2.3) and 19 of the limbs (table 2.4). My choice of which measurements to include was based on three main criteria; 1) their relevance to biological and ecological traits such as diet specialisation and locomotory adaptation, 2) their usefulness for assessing the overall shape and size of the specimen and 3) the ease with which they could be repeated both within and among specimens from different

species. Figures x-x depict the linear measurements of skulls and figures xx show the limb measurements.

I took each linear measurement three times, cycling through all 20 skull or 19 limb measurements then repeating the cycle to avoid measuring the same variable twice in a row. Small measurements (<2 mm) are particularly prone to high error rates (Cardini and Elton, 2008). Therefore, I took five separate replicates of some of the variables which were most prone to errors (marked with * in tables 2.3 and 2.4). These included four of the skull measurements (PWa, IncisorH, IFD and IFcanal) and five of the limb measurements (FemD, TibD, HumD, UlnD, RadD). Five replicates should give a more reliable median value because even if there are one or two outlying measurements there should be at least three replicates which are in close agreement (Cooper and Purvis, 2009).

TABLE 2.2: Mandibles' measurement abbreviations and descriptions. all taken from the labial (outer) side of the right jaw unless that side was broken or missing. All measurements were repeated three times except for those marked with * which were measured five times.

| Abbreviation | Measurement | Description |
|---------------------|----------------------------|--|
| ML | Mandible length | Maximum jaw length measured from the symphysis to the end of the jaw in a straight line to the condyloid crest/posterior notch |
| MTR | Mandible tooth row length | Anterior edge of the alveolus of the first tooth to the posterior edge of the alveolus of the last tooth on the same side |
| CorP | Coronoid process height | Perpendicular height from the top of the coronoid process to the base of the jaw bone |
| ConY | Condylloid height | Perpendicular height from the top of the mandibular condyle to the base of the jaw |
| CorCon | Coronoid-condylloid length | Diagonal distance from the coronoid tip to the condyloid crest/ posterior notch (Carraway <i>et al.</i> , 1996) |

TABLE 2.3: Skulls' measurement abbreviations and descriptions. All measurements were repeated three times except for those marked with * which were measured five times.

| Abbreviation | Measurement | Description |
|---------------------|----------------------------|--|
| CB | Condyllobasal length | Total skull length from the front of the premaxillary bones to the rear of the occipital condyles, measured from below |
| PL | Palate length | Maximum length of the palate from the anterior of the pre-maxilla to the posterior of the hard palate |
| TR | Tooth row length | From the front of the alveolus of the first incisor to the rear of the alveolus of the last molar on the same side |
| PWa* | Palate width anterior | Width across the palate measured between the posterior, outer-most points of the alveoli of the first pair of teeth |
| maxPW | Maximum palate width | Measured at the widest point of the palate |
| IncisorH* | Incisor height | Maximum height of the first incisor on the right |
| ZW | Zygomatic width | Maximum width between the zygomatic arches (measured within the arches from below the skull) |
| MX | Maxilla width | Width between the maxillary bones, measured from above the skull. Species with zygomatic arches; width from the innermost connection between the anterior of the arch and the skull. No arches; width between the anterior skull constrictions. |
| SQ | Squamosal width | Width between the squamosal bones, measured from above the skull. Species with zygomatic arches; width from the innermost connection between the posterior of the arch and the skull. No arches; width between the posterior skull constrictions |
| OL | Orbit length | Longitudinal length of the orbit opening measured along the edge of the skull from the maxilla to the squamosal. |
| IFD* | Interorbital foramen width | The maximum (vertical) diameter of the right interorbital foramen |
| IFW | Interorbital foramen width | Maximum width across the skull between the two interorbital foramina, measured from above |
| IFcanal | Interorbital foramen canal | Length of the right IF canal measured between the anterior and posterior openings from above |
| BW | Braincase width | Width across the braincase at the widest point of the skull |
| SkH | Skull height | Perpendicular height from the highest point on the braincase to the base of the skull |

TABLE 2.4: Limbs' measurement abbreviations and descriptions. All measurements were repeated three times except for those marked with * which were measured five times.

| Abbreviation | Measurement | Description |
|---------------------|---------------------------|---|
| Inn | Innominate length | Maximum longitudinal length of the pelvic bone measured in a straight line from the anterior tip to the posterior curve |
| Obt | Obturator foramen | Maximum diameter of the opening in the pelvic bone |
| FemL | Femur length | Length of the bone excluding the femoral head (i.e. length of the bone without the joint area) |
| FemD* | Femur diameter | Minimum width across the shaft of the bone |
| TibL | Tibia length | Maximum longitudinal length of the tibia |
| TibU | Tibia unfused length | Length of the tibia which is not fused with the fibula |
| TibD* | Tibia diameter | Minimum diameter across the shaft of the tibia bone |
| Foot | Foot length | Maximum length of the entire foot (heel to longest toe) |
| Toe | Toe length | Length of the longest toe bone (just the phalange bone up to the metatarsal joint) |
| ScapL | Scapula length | Perpendicular length of the scapula from the curved end to the anterior point |
| ScapW | Scapula width | Maximum perpendicular width across the bone |
| HumL | Humerus length | Maximum length of the bone. In golden moles (L-shaped humerus): diagonal distance between the two ends of the bone |
| HumLvert | Humerus length vertical | Only for golden moles with L-shaped humerus: length of the vertical (longer) side of the bone |
| HumLhori | Humerus length horizontal | Only for golden moles with L-shaped humerus: length of the horizontal (shorter) side of the bone |
| HumD* | Humerus diameter | Minimum diameter across the shaft of the humerus |
| UlnL | Ulna length | Length of the bone from the posterior tip to the wrist joint |
| RadL | Radius length | Length of the bone from the posterior tip to the wrist |
| UlnD* | Ulna diameter | Minimum diameter across the ulna |
| RadD* | Radius diameter | Minimum diameter across the radius |
| Hand | Hand length | Maximum length of the entire hand (wrist to longest finger) |
| Finger | Finger length | Length of the longest finger bone (to the metatarsal joint) |

2.2.4 Photographic set up

In order to get 2D landmarks for my specimens, I first had to photograph them. I used photographic copy stands consisting of a camera attachment with an adjustable height bar, a flat stage on which to place the specimen and an adjustable light source to either side of the stage. I used the copy stands that were available at each museum which differed in how the camera height was adjusted and in the light sources available. To take the light variability into account, on each day I took a picture of a white sheet of paper and used the custom white balance function on the camera to set the image as the baseline â€œwhiteâ€ measurement for those particular light conditions.

I photographed the specimens with a Canon EOS 650D camera fitted with either an EF 100mm f/2.8 Macro USM lens (skulls and limbs) or EFS 18-55mm lens (skins). I used a remote control (hähnel Combi TF) to take the photos to avoid shaking the camera and distorting the images. I photographed the specimens on a black material background. I placed the light source from the top left-hand corner of the picture and positioned a piece of white card on the bottom right side of the specimen which reflected the light back onto the specimen and minimised any shadows (figure 2.2 below).

I made small bean bags (12 x 5cm) from the same black material as the background and filled them with plastic beads. I used these bags as necessary to hold the specimens in position while being photographed. For example, when taking pictures of the lateral view of skulls, I placed one bean bag under the nose of the skull and another bag lying along the top (cranial) side of the skull to ensure that the side I was photographing lay in a flat plane relative to the camera and did not tilt in any direction. I used the grid-line function on the live-view display screen of the camera to position the specimens in the centre of each image.



FIGURE 2.2: Photographic set up for taking images of my skulls. The camera (above centre) is fitted to a copy stand, the light source is directed from the top-left corner of the image and the white card reflects the light back onto the skull.

2.2.5 Photographing specimens

I photographed the skulls in three views; dorsal (top of the cranium), ventral (underside of the skull with the palate roof facing uppermost) and lateral (right side of the skull). I also photographed the outer (buccal) side of the right mandible. When the right side of either the skull or mandibles were damaged or incomplete, I photographed the left sides and later reflected the images so

that they could be compared to pictures of the right sides (e.g. Barrow and Macleod, 2008).

Initially, I tried to take pictures of the limbs in similar orientations to the skulls (dorsal, ventral and lateral). However, there was considerable variation in how the limbs were preserved. For example, some limbs were still articulated while others had fragmented bones. It therefore proved impossible to place the limb bones in consistent orientations that would be comparable across species. Similarly, the small size of some limbs, combined with the frequently incomplete nature of postcranial museum collections, made landmark-based morphometric analyses of any limb pictures impractical. Therefore, I photographed the fore- and hind-limb bones in outer (the side facing away from the rest of the body) and inner (the side facing in towards the centre of the body) views for reference purposes only.

As I was limited by the maximum camera height available on the copy stands, most skins were too large to be photographed with the 100mm macro lens. Therefore, I used an EFS 18-55mm lens to take pictures of the skins. I photographed skins in the same three orientations as the skulls; dorsal (the upper surface of the animal), ventral (the belly side of the skin) and lateral (right flank of the animal with the skin held in position using bean bags). The dorsal and ventral views give very approximate estimates of the overall body shape of the animal. The lateral views are less biologically relevant since the taxidermic process is unlikely to produce specimens which represent the true body height of the animal.

2.2.6 Saving and processing images

Photographs were captured and saved in a raw file format. Before using the pictures for morphometric analyses, I converted the raw files to binary (grey scale) images and re-saved them as TIFF files. The black and white pictures

were more useful for later analyses since I was not interested in including any colour comparisons and it is easier to see some biological features in binary images. TIFF files were the most appropriate to use for my morphometric analyses as they are uncompressed (in comparison to JPEG) images and therefore there is less chance of any picture distortions which may affect later analyses (HERC, 2013).

2.3 GEOMETRIC MORPHOMETRIC ANALYSES

2.3.1 Landmark placement on images

I used a combination of landmark and semilandmark analysis approaches to assess the shape variability in my skull and mandible specimens specimens.

I used the TPS software suite (Rohlf, 2013) to digitise landmarks and curves on my pictures. I set the scale on each pictures individually to standardise for the different camera heights I used when photographing my specimens. I created separate data files for each of my four morphometric analyses (skulls in dorsal, ventral and lateral views and mandibles in lateral view). I digitised landmarks and semilandmark points on each picture individually.

When combining landmark and semi-landmark approaches, there is a potential problem of over-sampling the curves (REFS). To determine the number of semilandmark points required to adequately summarise the curves in my data sets, I followed the method outlined by MacLeod (2012). For each data set I chose a random selection of pictures of specimens which represented the breadth of the morphological data (i.e. specimens from each sub-group of species). I drew the appropriate curves on each specimen and over-sampled the number of points on the curves. I measured the length of the line and regarded that as the 100%, true length of that outline. I then re-sampled the curves with decreasing numbers of points and measured the length of the outlines. I cal-

culated the length of each re-sampled curve as a percentage of the total length of the curve and then found the average percentage length for that reduced number of semilandmark points across all of the specimens in my test file. I continued this process until I found the minimum number of points that gave a curve length which was at least 96% accurate. I repeated these curve-sampling tests for each analysis to determine the minimum number of semilandmark points which would give accurate representations of morphological shape.

Here I summarise the landmarks and curves which I used on each of my different sets of pictures. For landmarks which are defined by dental structures, I used published dental formulae (Nowak, 1983; MacPhee, 1987; Knox Jones and Manning, 1992; Marshall and Eisenberg, 1996; Nagorsen, 2002; Goodman *et al.*, 2006; Asher and Lehmann, 2008; ADW, 2013) where available to identify the number and type of teeth in each species.

2.3.2 Skulls: dorsal view

Most of my landmarks in this view are relative (type 3) points which represent overall morphological shape but not necessarily homologous biological features (Zelditch *et al.*, 2012). I placed ten landmarks and drew four semilandmark curves to represent the shape of both the braincase (posterior) and nasal (anterior) area of the skulls (figure 2.3). Table 2.5 describes how I placed the landmarks and drew the outline curves for my dorsal skull pictures

2.3.3 Skulls: ventral view

Most of the landmarks in this view are concentrated around the dentition and palate of the animals. I placed 13 landmarks and drew one outline curve (re-sampled to 60 semilandmark points) around the back of the skull between landmarks 12 and 13 (figure 2.4). The high variability of my species' basi-cranial region and difficulties associated with identifying developmentally or func-

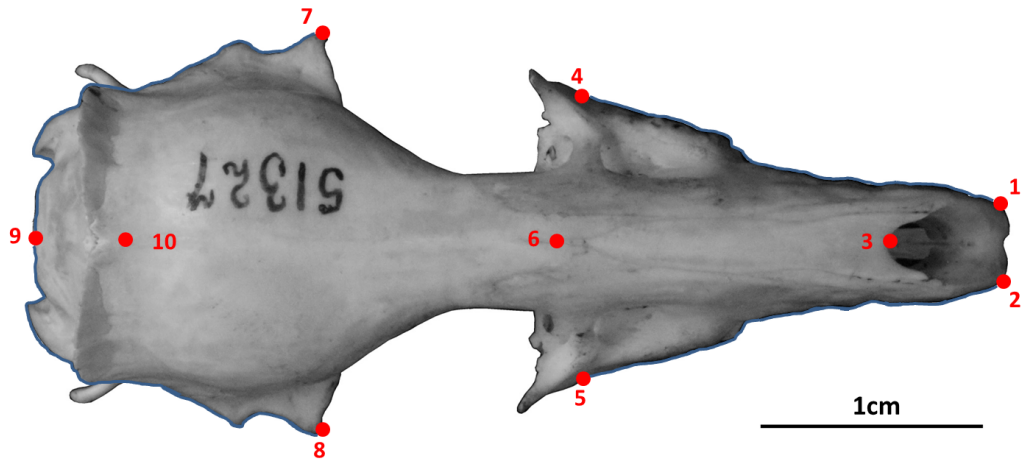


FIGURE 2.3: Landmarks (red) and curves (blue) for the skulls in dorsal view. Curves were re-sampled to the same number of evenly-spaced points. See table 2.5 for description of curves and landmarks. *Potamogale velox* (Tenrecidae) skull, museum accession number: AMNH_51327

tionally homologous points precluded designation of additional landmarks towards the back of the skulls. Table 2.6 outlines the descriptions of the landmarks I placed on the ventral pictures.

TABLE 2.5: Descriptions of the landmarks (points) and curves (semilandmarks) for the skulls in dorsal view (figure 2.3)

| Landmark | Description |
|-------------------------------|---|
| 1 + 2 | Left (1) and right (2) anterior points of the premaxilla |
| 3 | Anterior of the nasal bones in the midline |
| 4 + 5 | Maximum width of the palate (maxillary) on the left (4) and right (5) |
| 6 | Midline intersection between nasal and frontal bones |
| 7 + 8 | Widest point of the skull on the left (7) and right (8) |
| 9 | Posterior of the skull in the midline |
| 10 | Posterior intersection between sagittal and parietal sutures |
| Curve A (12 points) | Outline of the braincase on the left side, between landmarks 9 and 7 (does not include visible features from the lower (ventral) side of the skull) |
| Curve B (10 points) | Outline of the palate on the left side, between landmarks 4 and 1 (outline of the rostrum only, not the shape of the teeth) |
| Curve C (12 points) | Outline of the braincase on the right side, between landmarks 9 and 8 (does not include visible features from the lower (ventral) side of the skull) |
| Curve D (10 points) | Outline of the palate on the right side, between landmarks 5 and 2 (outline of the rostrum only, not the shape of the teeth) |

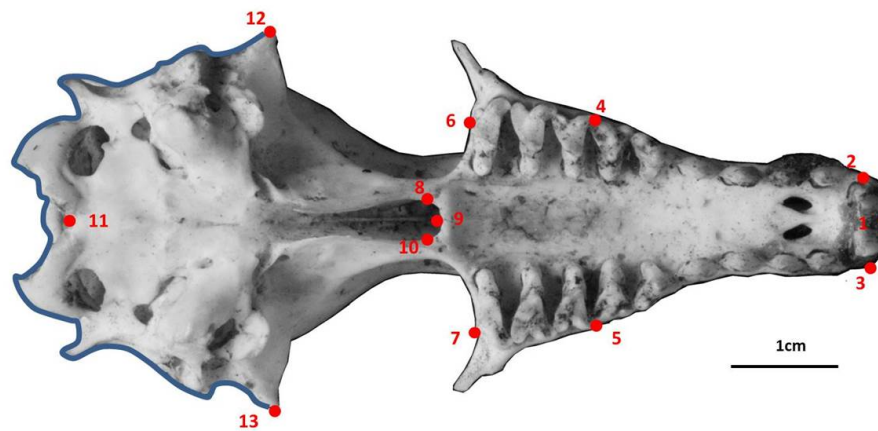


FIGURE 2.4: Landmarks (red) and curve (blue) for the ventral skull pictures, further descriptions in table 2.6. The specimen is a giant otter shrew tenrec, *Potamogale velox*, NHML 1934.6.16.2

2.3.4 Skulls: lateral view

I placed nine landmarks on the lateral pictures (see figure 2.5 below) and also drew two semilandmark curves between landmarks 7 and 8 to represent the

TABLE 2.6: Descriptions of the landmarks (points) and curves (semilandmarks) for the skulls in ventral view (figure 2.4)

| Landmark | Description |
|----------|---|
| 1 | Anterior point of the palate |
| 2 + 3 | Posterior, lateral extremity of the right (2) and left(3) incisor |
| 4 + 5 | Anterior, outer point of the first molar on the right (4) and left (5) |
| 6 + 7 | Posterior, outermost point of the molar surface on the right (6) and left (7) |
| 8 | Widest point of the curve of the palatine on the right side |
| 9 | Posterior point of the palatine in the midline |
| 10 | Widest point of the curve of the palatine on the left side |
| 11 | Anterior of the occipital foramen in the midline |
| 12 + 13 | Widest (extreme lateral) point of the braincase on the right (12) and left (13) |
| Curve* | Outline of the back of the skull (between landmarks 12 and 13), 60 points |

*NB: This curve doesn't necessarily trace homologous features because of the variation in the position of the foramen magnum.

shape of the back of the skull (resampled to 20 semilandmark points) and landmarks 8 and 1 (resampled to 15 semilandmark points) down the midline of the nose to represent the shape of the top of the skull. Table 2.7 describes my definitions for each of the landmark points. If specimens that were damaged on their right side I reflected photographs of the left lateral side of the skull so that all pictures would be in the same orientation. I originally tried to include more landmarks around the infraorbital foramina (IF) as a crude measure of facial sensitivity and because the IF area is correlated with ecotypes (Crumpton and Thompson, 2012). However, it proved impossible to see the boundaries of the IF in many species and single landmark points could not represent the shape of the full foramina.

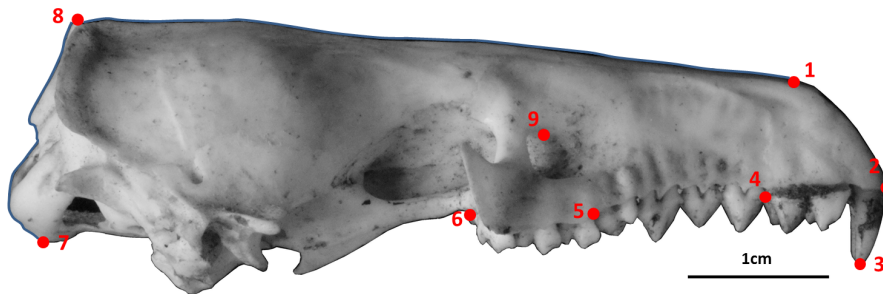


FIGURE 2.5: Landmarks (red) and curve (blue) for the lateral skull pictures, further descriptions in table 2.7. The specimen is a giant otter shrew tenrec, *Potamogale velox*, NHML 1934.6.16.2

TABLE 2.7: Descriptions of the landmarks (points) and curves (semilandmarks) for the skulls in lateral view (see Figure X).

| Landmark | Description |
|--------------------------------|---|
| 1 | Anterior, upper tip of the nasal bone |
| 2 | Anterior of the alveolus of the first incisor |
| 3 | Lowest point of the first incisor |
| 4 | Posterior of the alveolus of the last incisor |
| 5 | Anterior tip of the alveolus of the first molar |
| 6 | Posterior tip of the alveolus of the last molar |
| 7 | Lowest point of the basi-occipital (base of the back of the skull) |
| 8 | Highest point of the braincase |
| 9 | Highest point of the infraorbital foramen |
| Curve A (20 points) | Between points 7 and 8 Back of the skull from the lowest to highest points |
| Curve B (15 points) | Between points 8 and 1 From the highest point of the braincase to the front of the nasal |

2.3.5 Mandibles

I placed seven landmarks and drew four curves on each mandible picture (again, reflecting any pictures of the left mandible so they could be compared to pictures of the right side). I drew separate curves around each of the three processes of the ascending ramus; coronoid, condyloid and angular and along the base of the horizontal ramus of the jaw. While obviously part of an in-

CHAPTER 2

tegrated jaw unit, the development of the mandibular processes are also, in some aspects, independent since they attach different muscles which exert different masticatory forces on the jaw (Barrow and Macleod, 2008). Therefore, by drawing separate curves around each of these elements, my ensuing analyses could assess the relative shape changes of different components of the jaw with relevance to variation in feeding strategies and capabilities.

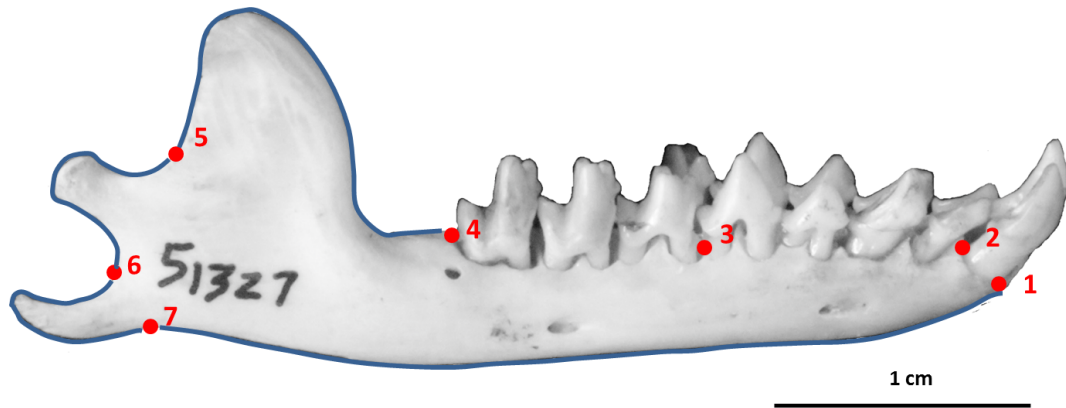


FIGURE 2.6: Landmarks (red) and curves (blue) used for the mandibles. Curves were re-sampled to the same number of evenly-spaced points. See table 2.8 for description of curves and landmarks. *Potamogale velox* (Tenrecidae) mandible, accession number: AMNH_51327

TABLE 2.8: Descriptions of the landmarks (points) and curves (semilandmarks) for the mandibles in lateral (buccal) view (figure 2.6)

| Landmark | Description |
|----------|--|
| 1 | Anterior of the alveolus of the first incisor |
| 2 | Posterior of the alveolus of the first incisor |
| 3 | Anterior of the alveolus of the first molar |
| 4 | Posterior of the alveolus of the last molar |
| 5 | Maximum curvature between the coronoid and condylar processes |
| 6 | Maximum curvature between the condylar and angular processes |
| 7 | Maximum curvature between the angular process and the horizontal ramus |
| Curve A | Condylloid process (between landmarks 4 and 5, 15 points) |
| Curve B | Condylar process (between landmarks 5 and 6, 15 points) |
| Curve C | Angular process (between landmarks 6 and 7, 15 points) |
| Curve D | Base of the jaw (between landmarks 7 and 1, 12 points) |

2.3.6 Procrustes superimposition

After creating my files with the landmarks and semilandmarks placed on each picture, I used TPSUtil (Rohlf, 2012) to create sliders files (Zelditch *et al.*, 2012)

to define which points were semilandmarks. I conducted all further morphometric analyses in R version 3.1.1 (R Core Team, 2014) within the geomorph package (Adams *et al.*, 2013). For each of the separate data sets, we used the gpagen function to run a general Procrustes alignment (Rohlf and Marcus, 1993) of the landmark coordinates while sliding the semilandmarks by minimising procrustes distance (Bookstein, 1997). We used these Procrustes-aligned coordinates of all specimens to calculate average shape values for each species which we then used for a principal components (PC) analysis with the plotTangentSpace function (Adams *et al.*, 2013).

2.4 ERROR CHECKING

My data are prone to a number of different error sources. These include 1) taxonomic identification which has not been updated to currently accepted terms, 2) specimen ID errors, 3) possible variation associated with sex and age class of individuals, 4) the accuracy and repeatability with which species traits are measured, 5) morphometric errors associated with photographing specimens and the placement of landmarks. I address each of these possible sources of error below.

2.4.1 Taxonomic

I recorded species names as they were written on museum specimen labels and then corrected them to match the taxonomy in Wilson and ReaderâŽs Mammal Species of the World (2005). For recently identified species, such as *Microgale jobihely* (Goodman *et al.*, 2006), which are not included in Wilson and Reader (2005), I used the taxonomy recorded on the labels.

2.4.2 Specimen ID

There were four specimens from the Smithsonian Institute that had species labels which did not match between skulls and skins with the same specimen ID numbers. The four skulls were labelled as *Hemicentetes semispinosus*. The corresponding skins were originally labelled as *H. semispinosus* but this was crossed out and changed to *H. nigriceps*. The re-labelled skins looked clearly different to the undisputed *H. semispinosus* skins and also look more similar to other pictures of *H. nigriceps*. Therefore, I made the assumption that the re-labelling of the skins as *H. nigriceps* represents the true taxonomy and I treated the corresponding skulls as *H. nigriceps*.

2.4.3 Specimen sex and age

Information about the sex and/or age of an individual is often missing from museum records. Mammalian species can often be identified as juveniles by looking for incomplete fusion of the crania and non-fully erupted dentition (REFS) However, age classification in tenrecs is difficult using these criteria; in some species, the last molar does not erupt fully until the first molar has been shed so the full dentition is never present at any one time (Nowak, 1983). It is also difficult to distinguish deciduous from permanent teeth in *Microgale* tenrecs (Asher and Lehmann, 2008) which has led to confusion and misidentification of juvenile forms as separate species (Olson *et al.*, 2004). I excluded any obvious juvenile specimens from my data set. Where specimens could not be obviously identified as juveniles I treated them all as equivalent adult forms. I included both male and female specimens in my data as significant sexual dimorphism in skull or body size has not been identified in any of my species (REFS Olson *et al.*, 2004).

2.4.4 Linear measurements

As mentioned above (section 2.2.3), I took three replicate measurements of most of my variables and five replicates of other variables. Some morphometric studies take replicate measurements of a trait and use the average value for further analyses (REFS). Rather than taking the mean of each of three (or five) measures, I used the median as it is less likely to be skewed by outliers and gives a more accurate representation of the true value of the trait (REFS?). Before extracting the median values I followed the protocol for assessing measurement error outlined by (Cooper and Purvis, 2009). This method assesses whether there is a reasonable correlation among the replicate measurements of the same variable. The error checking criteria are based on two calculations; the coefficient of variation and the percentage spread.

I calculated the coefficient of variation (standard deviation/mean*100) for each measurement. This value estimates the extent to which replicate measurements deviate from the mean. When the coefficient of variation was less than 5%, I accepted the median value as an accurate measurement of the size of the structure. If the coefficient of variation was greater than 5%, indicative of a low agreement between replicate measurements, I measured the percentage spread of the data. For variables measured three times, I calculated percentage spread as $[(\text{minimum difference between neighbouring measurements}) / (\text{range of measured values}) * 100]$. For variables that I measured five times, the differences between neighbouring values were calculated and labelled from smallest to largest as a, b, c, and d with the range of the measured values designated as e (Cooper and Purvis, 2009). For these variables, I calculated percentage spread as $[(a/e + b/e + c/e) * 100]$. Small percentage spread values indicate close agreement between repeated measurements. When percentage spread approaches 50% the data are evenly spread out and therefore there is no way of knowing whether the median value is an accurate measurement of the

trait (Cooper and Purvis, 2009). I chose to use 25% as a cut off point for accepting the accuracy of measured traits.

I used these error checking criteria to assess the accuracy of my repeated measurements of both skulls and limbs.

2.4.5 Potential morphometrics error

I used 2D morphometrics to compare the morphologies of the skulls (section 2.3). The small size of my specimens, combined with the number of specimens involved in my study made 3D imaging impractical. It takes roughly 1.5 hours for a good quality scan of each specimen so it would have taken me at least 550 hours to scan the 366 specimens that I photographed.

While 2D methods are an accepted means of comparing morphological shape (e.g. Adams *et al.*, 2004; Mitteroecker and Gunz, 2009), particularly for comparing skull morphologies of small mammals (e.g. Cardini, 2003; Panchetti *et al.*, 2008; White and Searle, 2008; Barrow and Macleod, 2008; Scalici and Panchetti, 2011), the inherent discrepancies associated with comparing three dimensional objects using two dimensional pictures do introduce some difficulties of possible distortion of the image (Arnqvist and Mårtensson, 1998). Similarly, human error with how landmarks are positioned on specimens could also introduce noise into further analyses. In contrast to detailed intraspecific work (REFS) photographic or landmark placement errors are unlikely to be significant in interspecific studies since one would expect that the morphological variation among species is large enough to be detected as a signal above any background noise associated with methodological error (REFS). Nevertheless, it is still important to assess measurement error in a morphometric data set to increase confidence in the outcome of final analyses. I identify two main sources of morphometric measurement error; specimen orientation and placement of landmarks.

Variation in the orientation of specimens for photography is one of the main sources of error in 2D morphometric studies (Adriaens, 2007). If specimens are not placed on a flat plane or in a consistent position relative to the camera, areas of the object which are tilted towards the camera will appear to be larger than reality, distorting any subsequent morphometric analyses of the shape. I used a random subset of skulls comprised of one representative from each of my 89 species to estimate the overall specimen orientation error in my photographic dataset. This subset included representatives from each tenrec and golden mole species along with samples from my comparative species (total of xx moles, xx shrews, xx hedgehogs ...) I took three sets of pictures of each view of the skulls and mandibles, cycling through the pictures so that the specimen was removed and re-positioned before every shot (Viscosi and Cortini, 2011).

2.4.6 Landmark placement

I placed the landmarks on each set of pictures so inter-observer variation is not an issue for my study. However, repeatability and reliability of my choice of landmarks could affect the final results of my analyses (Arnqvist and Mårtensson, 1998). I used a combined, nested approach to test for both orientation and landmark placement error (Arnqvist and Mårtensson, 1998; Barrow and Macleod, 2008). For each of the 89 specimens in my random subset of species, I photographed their skulls (dorsal, ventral and lateral views) and mandibles three times. I then copied these images and placed landmarks on 3 copies of each image. I used a nested mixed mode ANOVA to assess the measurement error of the Procrustes-superimposed coordinates. There were three factors in my ANOVA; specimen, photo (3 pictures of each specimen) and landmark trial (placed landmarks on 3 copies of each of my photos).

CHAPTER 3

DISPARITY IN TENRECS COMPARED TO THEIR CLOSEST RELATIVES

3.1 INTRODUCTION

3.2 METHODS

For each of the morphometric data sets (dorsal, ventral, lateral skulls and mandibles), I ran a general Procrustes alignment (section 2.3.6) of just my tenrec and golden mole specimens to compare morphological diversity in the two families. I used the principal components axes which accounted for 95 % of the cumulative variation to calculate four disparity metrics; the sum and product of the range and variance of morphospace occupied by each family (Brusatte *et al.*, 2008; Foth *et al.*, 2012; Ruta *et al.*, 2013). We also calculated morphological disparity directly from the Procrustes-superimposed shape data based on the sum of the squared inter-landmark distances among species pairs (SSqDist, Zelditch *et al.*, 2012).

I used two approaches to test whether tenrecs have significantly different morphologies compared to golden moles. The first was a comparison of morphospace occupation between the two groups with non parametric MANOVAs (Anderson, 2001) to test whether tenrecs and golden moles occupy significantly different areas of morphospace (e.g Serb *et al.*, 2011; Ruta *et al.*, 2013).

Secondly, I used pairwise permutation tests to test the null hypothesis that tenrecs and golden moles have equal disparity. If this hypothesis were true

then the designation of each species as belonging to either tenrecs or golden moles should be arbitrary because each group would have the same disparity. Therefore I permuted the data by assigning family identities at random to each specimen and calculated the differences in disparity for each of the new family groupings. I repeated these permutations 1000 times to generate a null distribution of the expected differences in family disparity. I compared the observed (true) measures of the differences in disparity between tenrecs and golden moles to these permuted distributions to test whether the families had significantly different levels of disparity.

The majority of tenrec species (19 out of 31 in my data) are members of the *Microgale* (shrew-like) genus which is notable for its relatively low phenotypic diversity (Soarimalala and Goodman, 2011; Jenkins, 2003). The strong similarities among these species may mask signals of higher disparity among other tenrecs. Therefore I repeated my family-level comparisons of disparity with a reduced data set that excluded the *Microgale* so that I could compare disparity within the remaining 12 tenrec species to disparity within the 12 species of golden moles.

3.3 RESULTS

When we compared tenrecs' cranial morphologies to their closest relatives we found a trend towards higher disparity in tenrecs than in golden moles. However, these apparent differences were only significant for some disparity metrics. In contrast, golden moles have more diverse mandible shapes than tenrecs which appears to be due to greater morphological variety in the posterior mandible strucutres of golden moles (section 3.3.2).

3.3.1 Morphological disparity in tenrecs and golden moles

Figures 3.1 depict the morphospace plots derived from our principal components analyses of average Procrustes-superimposed shape coordinates for each species in our skull and mandible data respectively. We used the principal components axes which accounted for 95% of the cumulative variation ($n = 7$, 8, 8 axes for the dorsal, ventral and lateral skull analyses respectively and $n = 12$ axes for the mandibles) to calculate the disparity of each family.

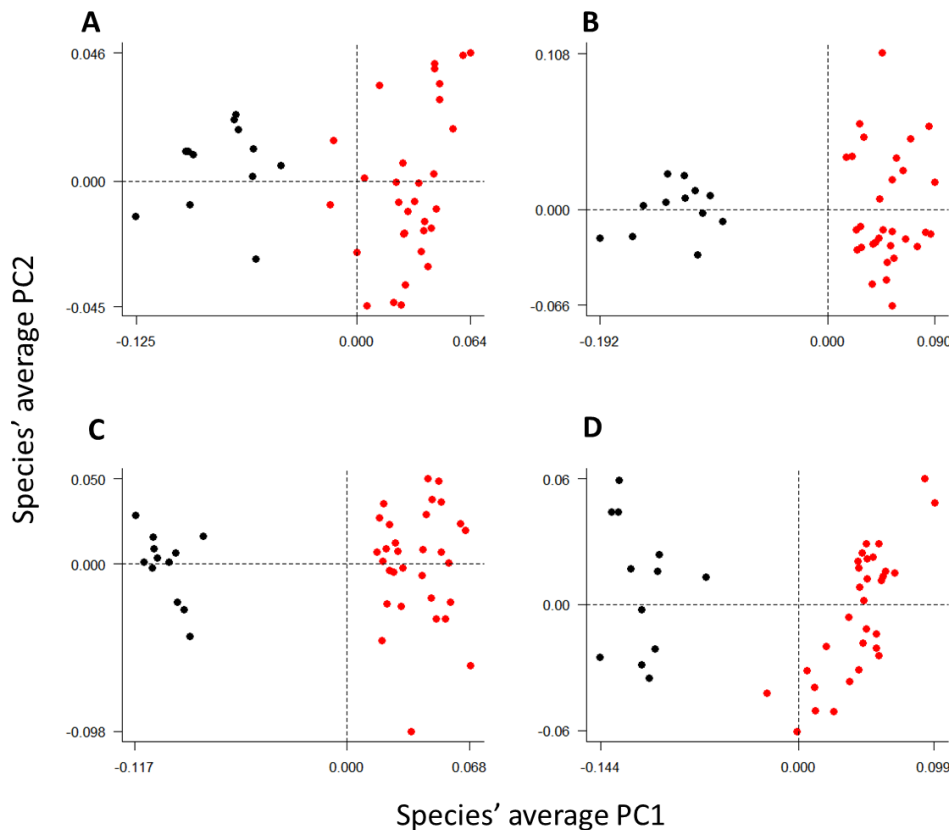


FIGURE 3.1: Principal components plots of the morphospaces occupied by tenrecs (red, $n=31$ species) and golden moles (black, $n=12$) for the skulls: dorsal (A), ventral (B), lateral (C) and mandibles (D) analyses. Axes are PC1 and PC2 of the average scores from a PCA analysis of mean Procrustes shape coordinates for each species.

Tenrecs and golden moles clearly have very different cranial and mandible morphologies: in each analysis, the families occupy significantly different areas of morphospace (npMANOVA, table 3.1).

TABLE 3.1: Summary of the npMANOVA comparisons of morphospace occupation for tenrecs and golden moles in each of the four analyses (three views of skulls and mandibles). In each case the two families occupy significantly different areas of morphospace.

| Analysis | F | R² | p value |
|-----------------|----------|----------------------|----------------|
| Skulls dorsal | 66.02 | 0.62 | 0.001 |
| Skulls ventral | 100.74 | 0.71 | 0.001 |
| Skulls lateral | 75.07 | 0.65 | 0.001 |
| Mandibles | 59.34 | 0.59 | 0.001 |

Our comparisons of disparity levels within each family yielded different trends for the skulls compared to the mandible analyses. In our analyses of the three different views of the skulls, when disparity is calculated from principal component - based metrics there is an overall trend for tenrecs to have higher disparity than golden moles. However, none of these differences are statistically significant (table 3.2). In contrast, when we calculated disparity based on the sum of squared interlandmark differences between species pairs (Zelditch *et al.*, 2012) then golden moles had significantly higher levels of disparity than tenrecs (table 3.2).

There is a less clear pattern from our analysis of disparity in the mandibles. Three of our five metrics indicate that golden moles have significantly higher disparity in the shape of their mandibles than tenrecs (table 3.2) although one metric (sum of ranges) indicated the opposite result.

The three curves that we placed at the back of the mandibles (figure 2.6) place a particular emphasis on shape variation in the posterior of the bone; the ramus, coronoid, condylar and angular processes. Therefore, higher disparity in golden mole mandibles compared to tenrecs could be driven by greater

TABLE 3.2: Summary of disparity comparisons between tenrecs (T) and golden moles (G) for each of the data sets(rows) and five disparity metrics (columns). "Mandibles:one curve" refers to my shape analysis of mandibles excluding the three curves around the posterior structures of jaw (figure 2.5). Significant differences are highlighted in bold with the corresponding p value in brackets. Disparity metrics are; sum of variance, product of variance, sum of ranges, product of ranges and sum of squared distances among species.

| Disparity metric | SumVar | ProdVar | SumRange | ProdRange |
|---------------------|--------|------------------------|------------------------|------------------------|
| Skulls dorsal | T>G | T>G | T>G | T>G |
| Skulls lateral | T>G | T>G | T>G | T>G |
| Skulls ventral | T>G | G>T | T>G | T>G |
| Mandibles | G>T | G>T* (0.008) | T>G* (0.025) | G>T* (0.009) |
| Mandibles:one curve | G>T | G>T | T>G | T>G |

morphological variation in these structures. To test this idea, we repeated our morphometric analyses of the mandibles with a reduced data set of points; just the seven landmark points and one single curve at the base of the jaw between landmarks 1 and 7 (figure 2.6). When we compared familial disparity levels with this reduced data set we found that golden moles no longer had significantly higher disparity than tenrecs but rather there were some indications that the opposite was true (table 3.2).

3.3.2 Morphological disparity in non-*Microgale* tenrecs and golden moles

We repeated our disparity comparisons with a subset of the tenrec specimens to remove the large and phenotypically similar *Microgale* tenrec genus. In this case we found that tenrecs have significantly higher disparity than golden moles when the skulls are analysed in lateral view (table 3.3). However, none of the other comparisons in any of the analyses were significant. Similarly, the trend in the main analysis for golden moles to have significantly higher disparity measured as the sum of squared inter-landmark distances (table 3.2) was not repeated in this comparison of disparity in non-*Microgale* tenrecs and golden moles (table 3.3).

TABLE 3.3: Summary of disparity comparisons between non-*Microgale* tenrecs (T) and golden moles (G) for each of the data sets(rows) and five disparity metrics (columns). Significant differences are highlighted in bold with the corresponding p value in brackets. Disparity metrics are; sum of variance, product of variance, sum of ranges, product of ranges and sum of squared distances among species.

| Disparity metric | SumVar | ProdVar | SumRange | ProdRange |
|-------------------------|------------------------|----------------|------------------------|-----------------------|
| Skulls dorsal | T>G | T>G | T>G | T>G |
| Skulls lateral | T>G* (0.014) | T>G | T>G* (0.001) | T>G*(0.003) |
| Skulls ventral | T>G | T>G | T>G | T>G |
| Mandibles | T>G | G>T | T>G | G>T |

3.4 DISCUSSION

CHAPTER 4

CONVERGENCE AMONG TENRECS AND OTHER SMALL MAMMALS

4.1 INTRODUCTION

4.2 METHODS

4.2.1 *Phylogeny*

Instead of basing my analyses on individual trees and assuming that their topologies are known without error (e.g. Ruta *et al.*, 2013; Foth *et al.*, 2012; Brusatte *et al.*, 2008; Harmon *et al.*, 2003) I used a distribution of 101 pruned phylogenies derived from the randomly resolved mammalian supertrees in (Kuhn *et al.*, 2011).

Eight species (six *Microgale* tenrecs and two golden moles) in my morphological data sets were not in the phylogenies. Phylogenetic relationships among the *Microgale* have not been resolved more recently than the (Kuhn *et al.*, 2011) analysis, therefore I added the additional *Microgale* species at random to the *Microgale* genus within each phylogeny (Revell, 2012). I could not use the same approach to add the two missing golden mole species because they were the only representatives of their respective genera within my data. Therefore I randomly added these species to the common ancestral node (using the find-MRCA function in phytools (Revell, 2012)) of all golden moles within each phylogeny. Adding these extra species to the phylogenies created polytomies which I resolved arbitrarily using zero-length branches (Paradis *et al.*, 2004). I

CHAPTER 4

calculated pairwise phylogenetic distances among species using the cophenetic function (R Core Team, 2014).

4.2.2 *Quantifying convergence*

4.3 RESULTS

4.4 DISCUSSION

CHAPTER 5

DISCUSSION

Overall summary of points and implications of findings

5.1 GENERAL DISCUSSION

5.2 POSSIBLE ISSUES

5.3 FUTURE DIRECTIONS

5.3.1 Measuring the adaptiveness of phenotypic traits

5.3.2 Evolutionary predictions of divergence and convergence

5.3.3 Ecological convergence

5.3.4 Studies of behavioural convergence

I have focused on morphological (phenotypic) similarities among tenrecs and other small mammals. These studies could be extended to tests of functional or behavioural convergences among tenrecs and other distantly related species. One particularly interesting extension would be to study echolocatory capabilities in tenrecs.

Gould 1965 demonstrated echolocatory abilities in three species of tenrec; *Echinops telfairi*, *Hemicentetes semispinosus* and *Microgale dobsoni*, indicating that they share behavioural similarities with some shrews (Gould *et al.*, 1964; Tomasi, 1979; Siemers *et al.*, 2009). Subsequent work demonstrated that the auditory range of *Echinops telfairi* includes ultrasonic frequencies (Drexel *et al.*, 2003) and

there have also been physiological investigations of stridulation behaviour in *Hemicentetes* tenrecs (Eisenberg and Gould, 1969; Endo *et al.*, 2010). However, aside from these studies echolocatory capabilities in tenrecs have not been investigated further. Recent studies have found evidence for sequence-level genomic convergence underlying independent origins of echolocation in multiple mammalian lineages (Parker *et al.*, 2013). Therefore, re-assessing and expanding behavioural echolocatory capabilities within tenrecs could be an important first step towards looking for further convergence at the genetic level.

I went to Madagascar in March/April 2014 as part of a research trip led by Dr. Steve Goodman to conduct behavioural tests of echolocation in *Microgale*. My aim was to record the sounds made by the animals as they moved through a wooden maze towards a food reward to determine whether there was evidence that they were using sounds to navigate through their environment. I tried multiple variations of our protocol but unfortunately none of the animals we tested produced any noise (17 individuals from 5 different species). However, it is clear that this negative result is a failure of the experimental design rather than an indication that *Microgale* don't navigate using sounds. My sample included *Microgale dobsoni* which is one of the few species that is known to echolocate from previous experiments (Gould, 1965). Similarly, other more experienced researchers in the group had heard the *Microgale* making sounds while foraging.

Previous studies of echolocation in small mammals (Gould *et al.*, 1964; Gould, 1965; Tomasi, 1979; Siemers *et al.*, 2009) all used captive individuals which were trained to perform specific tasks. Unfortunately such a prolonged procedure was not possible for me within constraints of time and facilities. However similar, more prolonged studies could reveal very interesting insights into echolocatory behaviour and capabilities within tenrecs. This work would also fit in with a more holistic view of understanding convergence among tenrecs and other

small mammals within morphological, ecological, behavioural and potentially genetic contexts.

5.4 CONCLUSIONS

BIBLIOGRAPHY

- Adams D., Otárola-Castillo E., and Paradis E. 2013. geomorph: an r package for the collection and analysis of geometric morphometric shape data. *Methods in Ecology and Evolution* 4:393–399.
- Adams D.C., Rohlf F.J., and Slice D. 2004. Geometric morphometrics: Ten years of progress following the "revolution". *Italian Journal of Zoology* 71:5–16.
- Adriaens D. 2007. Protocol for error testing in landmark based geometric morphometrics.
- ADW. 2013. Animal diversity web.
- Anderson M. 2001. A new method for non-parametric multivariate analysis of variance. *Austral Ecology* 26:32–46.
- Arnqvist G. and Mårtensson T. 1998. Measurement error in geometric morphometrics; empirical strategies to assess and reduce its impact on measures of shape. *Acta Zoologica Academiae Scientiarum Hungaricae* 44:73–96.
- Asher R. and Hofreiter M. 2006. Tenrec phylogeny and the noninvasive extraction of nuclear DNA. *Systematic Biology* 55:181–194.
- Asher R.J. and Lehmann T. 2008. Dental eruption in Afrotherian mammals. *BMC Biology* 6.
- Barrow E. and Macleod N. 2008. Shape variation in the mole dentary (Talpidae: Mammalia). *Zoological Journal of the Linnean Society* 153:187–211.
- Bookstein F. 1997. Landmark methods for forms without landmarks: morphometrics of group differences in outline shape. *Medical image analysis* 1:225–243.
- Brusatte S., Benton M., Ruta M., and Lloyd G. 2008. Superiority, competition and opportunism in the evolutionary radiation of dinosaurs. *Science* 321:1485–1488.
- Cardini A. 2003. The geometry of the marmot (Rodentia: Sciuridae) mandible: phylogeny and patterns of morphological evolution. *Systematic Biology* 52:186–205.
- Cardini A. and Elton S. 2008. Does the skull carry a phylogenetic signal? Evolution and modularity in the guenons. *Biological Journal of the Linnean Society* 93:813–834.

- Carraway L., Verts B., Jones M., and Whitaker J. 1996. A search for age-related changes in bite force and diet in shrews. *American Midland Naturalist* 135:231–240.
- Cooper N. and Purvis A. 2009. What factors shape rates of phenotypic evolution? A comparative study of cranial morphology of four mammalian clades. *Journal of Evolutionary Biology* 22:1024–1035.
- Crumpton N. and Thompson R. 2012. The holes of moles: Osteological correlates of the trigeminal nerve in Talpidae. *Journal of Mammalian Evolution*.
- Drexel M., Faulstich M., Von Stebut B., Radtke-Schuller S., and Kössl M. 2003. Distortion product otoacoustic emissions and auditory evoked potentials in the hedgehog tenrec, *Echinops telfairi*. *Journal of the Association for Research in Otolaryngology* 4:555–564.
- Eisenberg J.F. and Gould E. 1969. The Tenrecs: A Study in Mammalian Behaviour and Evolution. *Smithsonian Contributions to Zoology* 27:1–152.
- Endo H., Koyabu D., Kimura J., Rakotondraparany F., Matsui A., Yonezawa T., Shinohara A., and Hasegawa M. 2010. A quill vibrating mechanism for a sounding apparatus in the streaked tenrec (*Hemicentetes semispinosus*). *Zoological science* 27:427–432.
- Foth C., Brusatte S., and Butler R. 2012. Do different disparity proxies converge on a common signal? Insights from the cranial morphometrics and evolutionary history of *Pterosauria* (Diapsida: Archosauria). *Journal of Evolutionary Biology* 25:904–915.
- Gavrilets S. and Losos J. 2009. Adaptive radiation: contrasting theory with data. *Science* 323:732–736.
- Glor R. 2010. Phylogenetic insights on adaptive radiation. *Annual Review of Ecology, Evolution, and Systematics* 41:251–270.
- Goodman S.M., Raxworthy C.J., Maminirina C.P., and Olson L.E. 2006. A new species of shrew tenrec (*Microgale jobihely*) from northern Madagascar. *Journal of Zoology* 270:384–398.
- Gould E. 1965. Evidence for echolocation in the Tenrecidae of Madagascar. *Proceedings of the American Philosophical Society* 109:352–360.
- Gould E. and Eisenberg J.F. 1966. Notes on the biology of the Tenrecidae. *Journal of Mammalogy* 47:660–686.
- Gould E., Negus N., and Novick A. 1964. Evidence for echolocation in shrews. *The Journal of Experimental Zoology* 156:19–37.

BIBLIOGRAPHY

- Harmon L., Schulte J., Larson A., and Losos J.B. 2003. Tempo and mode of evolutionary radiation in iguanian lizards. *Science* 301:961–964.
- HERC U.B. 2013. RHOI Fossil Photography Protocol.
- Jenkins P. 2003. *Microgale, shrew tenrecs*, pages 1273–1278. The University of Chicago Press, Chicago.
- Knox Jones J. and Manning R. 1992. Insectivores.
- Kuhn T., Mooers A., and Thomas G. 2011. A simple polytomy resolver for dated phylogenies. *Methods in Ecology and Evolution* 2:427–436.
- Losos J. and Miles D. 2002. Testing the hypothesis that a clade has adaptively radiated: Iguanid lizards as a case study. *The American Naturalist* 160:147–157.
- Losos J.B. and Mahler D. 2010. Adaptive radiation: the interaction of ecological opportunity, adaptation and speciation, chap. 15, pages 381–420. Sinauer Association, Sunderland, MA.
- MacLeod N. 2012. Going Round the Bend ii: Extended Eigenshape Analysis.
- MacPhee R. 1987. The shrew tenrecs of Madagascar: Systematic revision and holocene distribution of *Microgale* (Tenrecidae, Insectivora). *American Museum Novitates Number 2889*:1–45.
- Marshall C. and Eisenberg J.F. 1996. *Hemicentetes semispinosus*.
- Mitteroecker P. and Gunz P. 2009. Advances in geometric morphometrics. *Evolutionary Biology* 36:235–247.
- Nagorsen D. 2002. An identification manual to the small mammals of British Columbia.
- Nowak R. 1983. *Walker's Mammals of the World*, 4th edition, vol. 1. Johns Hopkins University Press, Baltimore.
- Olson L. and Goodman S. 2003. Phylogeny and biogeography of tenrecs, pages 1235–1242. The University of Chicago Press, Chicago.
- Olson L., Goodman S., and Yoder A. 2004. Illumination of cryptic species boundaries in long-tailed shrew tenrecs (Mammalia: Tenrecidae; *Microgale*), with new insights into geographic variation and distributional constraints. *Biological Journal of the Linnean Society* 83.
- Olson L.E. 2013. Tenrecs. *Current Biology* 23:R5–R8.
- Olson M.E. and Arroyo-Santos A. 2009. Thinking in continua: beyond the “adaptive radiation” metaphor. *BioEssays* 31:1337–1346.

- Panchetti F., Scalici M., Carpaneto G., and Gibertini G. 2008. Shape and size variations in the cranium of elephant-shrews: a morphometric contribution to a phylogenetic debate. *Zoomorphology* 127:69–82.
- Paradis E., Claude J., and Strimmer K. 2004. Ape: Analyses of Phylogenetics and Evolution in R language. *Bioinformatics* 20:289–290.
- Parker J., Tsagkogeorga G., Cotton J., Liu Y., Provero P., Stupka E., and Rossiter S. 2013. Genome-wide signatures of convergent evolution in echolocating mammals. *Nature* .
- Poux C., Madsen O., Glos J., de Jong W.W., and Vences M. 2008. Molecular phylogeny and divergence times of Malagasy tenrecs: Influence of data partitioning and taxon sampling on dating analyses. *BMC Evolutionary Biology* 8.
- R Core Team. 2014. R: A Language and Environment for Statistical Computing. R Foundation for Statistical Computing, Vienna, Austria.
- Revell L. 2012. phytools: an R package for phylogenetic comparative biology (and other things). *Methods in Ecology and Evolution* 3:217–223.
- Rohlf F. 2012. Tpsutil.
- Rohlf F. 2013. Tpsdig2 ver 2.17.
- Rohlf J. and Marcus L. 1993. A revolution in morphometrics. *Trends in Ecology & Evolution* 8:129–132.
- Ruta M., Angielczyk K., Fröbisch J., and Benton M. 2013. Decoupling of morphological disparity and taxic diversity during the adaptive radiation of anomodont therapsids. *Proceedings of the Royal Society B: Biological Sciences* 280:20131071.
- Scalici M. and Panchetti F. 2011. Morphological cranial diversity contributes to phylogeny in soft-furred sengis (Afrotheria, Macroscelidea). *Zoology* 114:85–94.
- Serb J., Alejandrino A., Otárola-Castillo E., and Adams D. 2011. Morphological convergence of shell shape in distantly related scallop species (mollusca: Pectinidae). *Zoological Journal of the Linnean Society* 163:571–584.
- Siemers B., Schauermann G., Turni H., and von Merten S. 2009. Why do shrews twitter? communication or simple echo-based orientation. *Biology Letters* 5:593–596.
- Soarimalala V. and Goodman S. 2011. Les petits mammifères de Madagascar. Guides sur la diversité biologique de Madagascar, Association Vahatra, Antananarivo, Madagascar.

BIBLIOGRAPHY

- Stanhope M., Waddell V., Madsen O., de Jong W., Hedges S., Cleven G., Kao D., and Springer M. 1998. Molecular evidence for multiple origins of insectivora and for a new order of endemic african insectivore mammals. *Proceedings of the National Academy of Sciences* 95:9967–9972.
- Symonds M.R.E. 2005. Phylogeny and life histories of the "Insectivora": controversies and consequences. *Biological Reviews* 80:93–128.
- Tomasi T.E. 1979. Echolocation by the short-tailed shrew *Blarina brevicauda*. *Journal of Mammalogy* 60:751–759.
- Viscosi V. and Cortini A. 2011. Leaf morphology, taxonomy and geometric morphometrics: a simplified protocol for beginners. *PLOS One* 6:e25630.
- White T. and Searle J. 2008. Mandible asymmetry and genetic diversity in island populations of the common shrew, *Sorex araneus*. *Journal of Evolutionary Biology* 21:636–641.
- Wilson D. and Reeder D. 2005. *Mammal species of the world. A taxonomic and geographic reference* (3rd ed). Johns Hopkins University Press.
- Zelditch M., Swiderski D., and Sheets D. 2012. *Geometric Morphometrics for Biologists*, second edition. Academic Press, Elsevier, United States of America.